



P-084

Seismic attenuation across a BSR in the Makran offshore

Kalachand Sain, Anoop Kumar Singh, NGRI*

Summary

The estimation of Q is important for qualifying whether a BSR is related to gas hydrates and free-gas. This property is also useful for identifying gas hydrates where detection of BSR is dubious. Here, we calculate the interval Q for three submarine sedimentary layers bounded by seafloor, BSR, one reflector above and another reflector below the BSR at three locations with moderate, strong and no BSR along a seismic line in the Makran accretionary prism for studying attenuation ($Q-1$) characteristics of sediments. Interval Q for hydrate-bearing sediments above the BSR are estimated as 191 ± 11 , 223 ± 12 , and 117 ± 5 , whereas interval Q for the underlying gas-bearing sediments are calculated as 112 ± 7 , 107 ± 8 and 124 ± 11 at moderate, strong and no BSR locations, respectively. The large variation in Q is observed at strong BSR. Thus Q can be used for ascertaining whether the observed BSR is due to gas hydrates, and for identifying gas hydrates at places where detection of BSR is rather doubtful. Interval Q of 98 ± 4 , 108 ± 5 , and 102 ± 5 respectively at moderate, strong and no BSR locations for the layer immediately beneath the seafloor show almost uniform attenuation.

Keywords: seismic quality factor; gas hydrates; free-gas; Makran accretionary prism.

Introduction

Gas hydrates are found in shallow sediments in deep-water regions in the outer continental margins, and have created interest due to their natural occurrences, role in climate change (methane being a green house gas) and submarine hazards such as the slope failure, and potential as major future energy resource (Klauda and Sandler, 2005; Sain and Gupta, 2008; Sain and Ojha, 2008). Hence, detection and quantitative assessment of gas-hydrates are important for the evaluation of energy potential and assessment of environment-hazard. The BSR, the most commonly used marker for gas hydrates, is an interface between gas hydrate-bearing sediments above and free gas-bearing sediments below. The sediments containing gas hydrates and free-gas can be characterized by physical properties like the seismic velocity and resistivity, and seismic attributes such as the blanking, reflection strength and instantaneous frequency etc. (Ojha and Sain, 2009). Another important property to characterize the gas hydrate- and free gas-bearing sediments is the seismic attenuation or quality factor (Sain et al., 2009). Gei and Carcione (2003) show in their model study that attenuation decreases or Q increases with increasing concentration of gas hydrates due to stiffening of sediments. By employing the logarithm

spectral ratio (LSR) method to the surface seismic reflection data, Sain et al. (2009) have demonstrated that the hydrate-bearing sediments are associated with high Q or low attenuation compared to that of normal (without hydrates) oceanic sediments.

The BSRs are wide-spread on seismic data in the Makran accretionary prism (Sain et al., 2000). Studies of seismic attributes (Ojha and Sain, 2009) and the velocity anomaly (Sain et al. 2000) favor the presence of gas hydrates and free gas across the BSR in the Makran offshore. Here we calculate the seismic interval Q at few CDP locations along a seismic line with a view to understanding the attenuation characteristics of gas hydrate- and free gas-bearing sediments, which can help predict whether the BSR is related to gas hydrates and underlying free-gas.

Methodology

The best known method for estimating Q from surface seismic reflection data of a 1-D multilayered earth is probably the LSR method (Sain et al., 2009) where the logarithm of spectral ratio of vertical reflections from two different reflectors with reflection times t_1 and t_2 is calculated as



$$\ln \left| \frac{A(f)_2}{A(f)_1} \right| = \ln \frac{G_2}{G_1} \left| \frac{C_2(f)}{C_1(f)} \right| - \pi \left[\frac{t_2}{Q_{av2}} - \frac{t_1}{Q_{av1}} \right] f \quad (1)$$

Subscripts 1 and 2 denote the first and second layers respectively. G accounts for the geometrical spreading and C takes into account the effects of reflection and transmission at boundaries. Q_{av2} and Q_{av1} are the average Q values from the source to the first and second layers respectively. The LSR against f as per equation (1) represents a straight line with slope, m as

$$m = -\pi \left[\frac{t_2}{Q_{av2}} - \frac{t_1}{Q_{av1}} \right] \quad (2)$$

From above equation we derive Q_{av2} as

$$Q_{av2} = \frac{\pi t_2 Q_{av1}}{\pi t_1 - m Q_{av1}} \quad (3)$$

The average and interval Q for the first layer is the same and thus we can calculate the Q_{av2} from equation (3). The Q between t_2 and t_1 , defined as the interval quality factor, Q_{int} , can be calculated using the equation of Zhang and Ulrich (2002) as

$$Q_{int} = \frac{t_2 - t_1}{Q_{av2}^{-1} t_2 - Q_{av1}^{-1} t_1} \quad (4)$$

Following this LSR method, we can calculate the Q_{int} for all subsequently deeper layers of a multilayered earth.

Application and Results

The method of estimating interval Qs from field data has been described in details by Sain and Singh (2011). They have applied to seismic data along a line in the Makran accretionary prism at three CDP locations (4286, 4372 and 4524) where the BSR is moderate, strong and absent (Fig.1a). The CDP has 24 traces with 100 m separation, and the nearest trace lies at 200 m offset. The data processing had been done using PROMax-2D and the sequence included a bandpass filter (4-8-50-60 Hz), spherical divergence correction ($1/(\text{time} \times \text{velocity}^2)$), minimum phase spiking deconvolution, detailed velocity analysis at every 10th CDP intervals, normal moveout (NMO)

correction and trace equalization. The NMO corrected seismic gather at CDP 4372 is shown in (Fig.1b). We calculate the amplitude spectra around four reflectors at seafloor, reflect-1 below the seafloor, the BSR and reflect-2 below the BSR. The LSR method requires the source signature. Since the attenuation ($Q=10,000$) through the water column is almost negligible, we assume the seafloor reflection as a reference signal in absence of source signature. Natural logarithms of spectral ratios of reflections from reflect-1, BSR and reflect-2 with reference to the seafloor reflection are used for calculating the slopes as per equation (1). Since the Q for water and the reflection times of seafloor, reflect-1, BSR and reflect-2 are known, the average Q_x at an offset, x upto reflect-1, BSR and reflect-2 can be calculated using equation (3). Sain et al. (2009) showed that Q_x decreases exponentially with offset as

$$\ln Q_x = \ln Q_0 - kx \quad (5)$$

where k is a constant and Q_0 is the average Q at zero-offset for the vertically traveling wave, which we are looking for. By extrapolating back to zero-offset according to equation (5), we can calculate the average Q_0 up to the reflect-1, BSR, reflect-2. The errors in field data are mapped into mean error, $\delta(Q_0)$ in estimated average Q_0 , which is determined according to following equation derived by Sain et al. (2009)

$$\delta(Q_0) = Q_0 \delta(\ln Q_0) \quad (6)$$

The Q_{int} between two successive reflectors is then calculated using the equation (4). The mean error, $\delta(Q_{int})$ in estimated Q_{int} is then determined using the following equation as

$$\delta Q_{int} = \frac{(t_2 - t_1)(Q_{av1}^2 t_2 \delta Q_{av2} - Q_{av2}^2 t_1 \delta Q_{av1})}{(t_2 Q_{av1} - t_1 Q_{av2})^2} \quad (7)$$

The interval Q and associated error for sedimentary formations between seafloor to reflect-1, reflect-1 to BSR, and BSR to reflect-2 at strong BSR (CDP 4372) are calculated as 108 ± 5 , 223 ± 12 , and 107 ± 8 respectively. The interval Q and associated error for sedimentary layers bounded by these reflectors are calculated as 98 ± 4 , 191 ± 11 and 112 ± 7 at moderate BSR, and 102 ± 5 , 117 ± 5 , and 124 ± 11 at no BSR, respectively. The estimated Q in the hydrate-bearing sediment is comparable to Q estimated for



hydrate-bearing sediments in other environments (Petersen et al., 2007; Sain et al., 2009). The interval Q versus TWT 1-D models are superimposed in Fig.2 over the respective CDP gathers from which the interval Q are derived using the LSR method.

Conclusions

The study reveals a three-layered Q -structure of shallow sediments in the deep water region in the Makran offshore. The Q_{int} of the first sedimentary layer shows almost uniform variation from 98 to 108 to 102 at CDPs 4286, 4372 and 4524 respectively along the line. We observe a large lateral change in Q_{int} for the second layer immediately above the BSR from 191 to 223 to 117 at locations where the BSR is moderate, strong and absent. The Q_{int} , estimated as 102, 117 and 124, respectively for three layers at CDP 4524 where the BSR is absent, shows a gradual increase due to increase in pressure downward, and can be considered as the background (without gas hydrates and free-gas) Q . Near the strong BSR, we find a sudden increase in Q_{int} from 108 to 223 at the BSR, followed by a large drop in Q_{int} to 107. This can be explained by the presence of large amount of gas hydrates above and free gas below the BSR. The moderate BSR at CDP 4286 is associated with moderate increase in Q_{int} from 98 to 191 at the BSR, followed by a drop to 112. This may indicate moderate amount of gas hydrates and less amount of free gas across the BSR. The calculation of Q can explain the strength of a BSR along a seismic line. Like velocity, the Q can also be used for the quantification of gas hydrates. The study of attenuation is also useful for the detection of gas hydrates in areas where identification of BSR becomes rather difficult due to parallel bedding. Besides characterizing the sediments, the estimated Q can be used to design an inverse Q filter to compensate the effects of attenuation for producing improved structural images of BSR and other reflectors of the shallow submarine sediments.

Acknowledgements

The authors are grateful to the Director, NGRI for his permission to publish this work. The Ministry of Earth Sciences, Govt. of India is thankfully acknowledged for sponsoring the gas- hydrates research at NGRI.

References

- Gei, D., Carcione, J.M., 2003. Acoustic properties of sediments saturated with gas hydrate, free gas and water. *Geophysical Prospecting* 51, 141-157
- Klauda, J.B., Sandler, S.I., 2005. Global distribution of methane hydrate in ocean sediment. *Energy and Fuels* 19, 459-70.
- Ojha, M., Sain, K., 2009. Seismic attributes for identifying gas hydrates and free-gas zones: application to the Makran accretionary prism. *Episodes* 32, 264-270.
- Petersen, C.J., Papenberg, C., Klaeschen, D., 2007. Local seismic quantification of gas hydrates and BSR characterization from multi-frequency OBS data at northern Hydrate Ridge. *Earth and Planetary Science Letters* 255, 414-431.
- Sain, K., Minshull, T.A., Singh, S.C., Hobbs, R.W., 2000. Evidence for a thick free gas layer beneath the bottom simulating reflector in the Makran accretionary prism. *Marine Geology* 164, 3-12.
- Sain, K., Gupta, H.K., 2008. Gas hydrates: Indian scenario. *Journal of Geological Society of India* 72, 299-311.
- Sain, K., Ojha, M., 2008. Identification and quantification of gas hydrates: a viable source of energy in the 21st century. *Memoir Geological Society of India* 68, 273-288.
- Sain, K., Singh, A.K., Thakur, N.K., Khanna, R.K., 2009. Seismic quality factor observations for gas-hydrate-bearing sediments on western margins of India. *Marine Geophysical Researches* 30, 137-145.
- Sain K., Singh, A.K., 2011. Seismic quality factors across a bottom simulating reflector in the Makran accretionary prism, *Marine & Petroleum Geology*, doi:10.1016/j.marpetgeo.2011.03.013, in press.
- Zhang, C. Ulrych, T.J., 2002. Estimation of Q from CMP records. *Geophysics* 67, 1542-1547.



Seismic attenuation across a BSR in the Makran offshore



"HYDERABAD 2012"

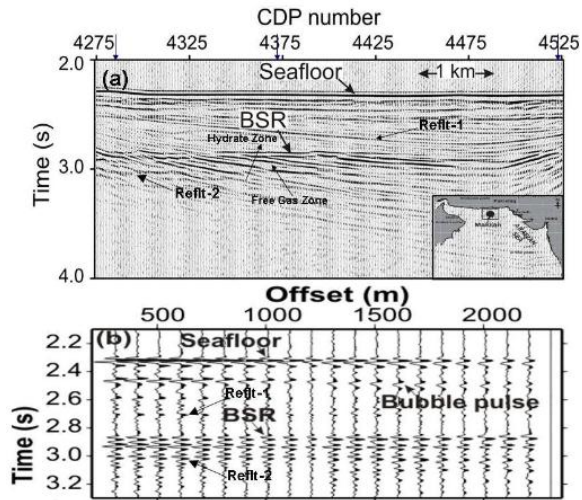


Fig.1(a). Seismic stack section along a north-south seismic line (inset shows the study area in the Makran accretionary prism). Amplitude spectra have been calculated around four reflectors: seafloor, reflect-1, BSR and reflect-2. (b) NMO corrected CDP gather at CDP 4372, showing the reflections at various offsets from the said four reflectors.

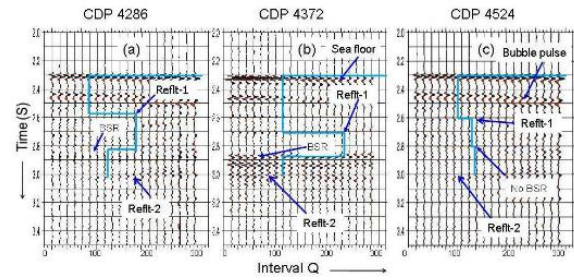


Fig.2. Field seismic gathers at CDPs 4286, 4372, and 4524, respectively, each superimposed with estimated interval Q.